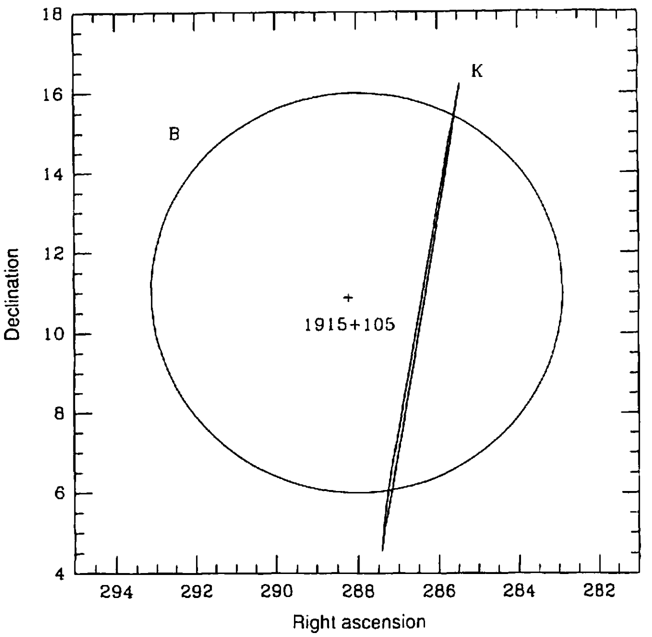

FIG. 3 Sky-map of the region near $\alpha = 288°$, $\delta = +11°$. The large circle (B) represents the average location of the three BATSE events. The size of this circle (~5°) reflects mainly the statistical errors of the three measured positions. Burst locations are obtained from the relative strength of their signals in the relevant subset of the eight identical Large Area Detectors (LADs). The position determination includes the detailed spectral dependence of the angular sensitivity of the detectors, and corrections for photon back-scattering by the Earth's atmosphere[23]. The diamond (K) represents the 2σ error box of SGR1900+14 (E. Mazets, personal communication). The small cross shows the location of the recently discovered[18,19] transient X-ray source GRS1915+105 (accuracy ~3′).

before the first SGR trigger and remained at maximum during the subsequent two triggers. Are the BATSE events related to the X-ray transient? For both the transient and SGR1900+14 the probability of being located inside the BATSE error box by chance is fairly small (~0.2% for assumed uniform sky distribution). As the positions for both SGR1900+14 and the transient are known with high accuracy (of the order of arcminutes) and they differ by more than ~1.5°, the KONUS events cannot be related to the Aquila transient. Moreover, a recent analysis[20] indicates that there was no persistent X-ray emission (upper limit of ~100 μJy) from this region in the sky, during the 1979 SGR bursts. We conclude that it is improbable that the BATSE events originate from GRS1915+105.

Our results suggest that burst activity from the 'old' SGR1900+14 has been detected again ~13 years after its discovery. If our detection is indeed the recurrence of activity from this source, it shows that SGRs keep their ability to be active for many years. The extended duration of SGR activity strengthens the argument that these sources are related to galactic (possibly population I) objects, plausibly neutron stars[4,5]. Recurrent SGR emissions do not signify a unique (catastrophic) event in the life cycle of the source, as is the case in the cosmological models currently favoured for the classical γ-ray bursts[21,22]. If on the other hand, the new SGR is not related to the SGR1900+14, the case for the SGRs to be associated with population I objects becomes even stronger than it was before, with four (rather than three) sources following their distribution. This is very different from recent results on classical γ-ray bursts, for which a galactic disc origin is excluded[6,21,22]. The long-term monitoring capability of BATSE gives hope of obtaining valuable information on the recurrence timescale of SGRs and (combined with other spacecraft) accurate source positions, which may lead to a better understanding of the nature of these objects. □

Received 4 January; accepted 9 March 1993.

1. Hurley, K. presented at *Taos Gamma-Ray Stars Conf* (1986).
2. Atteia, J.-L. *et al. Astrophys. J.* **320**, L105-110 (1987).
3. Laros, J. P. *et al. Astrophys. J.* **320**, L111-115 (1987).
4. Kouveliotou, C. *et al. Astrophys. J.* **322**, L21-25 (1987).
5. Norris, J. P. *et al. Astrophys. J.* **366**, 240-252 (1991).
6. Meegan, C. A. *et al. Nature* **355**, 143-145 (1992).
7. Fishman, G. J. *et al.* in *Proc. Gamma Ray Observatory Science Workshop* (ed. Johnson, W. N.) 39-50 (NASA/GSFC, Greenbelt, 1989).
8. Mazets, E. P., Golenetskii, S. V. & Guryan, Yu. A. *Sov. Astr. Lett.* **5**(6), 343-344 (1979).
9. Mazets, E. P. *et al. Astr. Space Sci.* **80**, 1-143 (1981).
10. Cline, T. L. *Ann. N.Y. Acad. Sci.* **375**, 314-329 (1981).
11. Lewin, W. H. G., van Paradijs, J. & Taam, R. E. in *X-Ray Binaries* (eds Lewin, W. H. G., van Paradijs, J. & van den Heuvel, E. P. J.) (in the press).
12. Schaefer, B. E. *et al. Astrophys. J.* **393**, L51-L54 (1992).
13. Band, D. *et al. Astrophys. J.* (submitted).
14. Golenetskii, S. V. *et al. Nature* **307**, 41-42 (1984).
15. Kouveliotou, C. *et al.* in *The Compton Observatory Science Workshop*, NASA CP-3137 (eds Shrader, C. R., Gehrels, N. & Dennis, B.) 61-68 (1992).
16. Lingenfelter, R. E. & Higdon, J. C. *Astrophys. J.* **397**, 576-578 (1992).
17. van Paradijs, J. *et al.* in *Proc. Compton Symp., St. Louis* (ed. Gehrels, N. (in the press).
18. Castro-Tirado, A. J. *et al. IAU Circ.* No. 5590 (1992).
19. Cordier, B. *et al.* in *Proc. Compton Symposium, St. Louis* (ed. Gehrels, N.) (in the press).
20. Lochner, J. & Whitlock, L. *IAU Circ.* No. 5658 (1992).
21. Paczynski, B. *Acta astr.* **41**, 157-166 (1991).
22. Paczynski, B. *Acta astr.* **41**, 257-267 (1991).
23. Brock, M. N. *et al.* in *Gamma Ray Bursts: Huntsville, AL, 1991* (eds Paciesas, W. S. & Fishman, G. J.) 383-387 (AIP, New York, 1992).

ACKNOWLEDGEMENTS. J.v.P. thanks the BATSE group at the Marshall Space Flight Center and the University of Alabama in Huntsville for their hospitality. He acknowledges financial support from the Leids Kerkhoven Bosscha Fonds.

Discovery of the candidate Kuiper belt object 1992 QB_1

David Jewitt* & Jane Luu†

* Institute for Astronomy, University of Hawaii, 2680 Woodlawn Drive, Honolulu, Hawaii 96822, USA
† Department of Astronomy, 601 Campbell Hall, University of California at Berkeley, Berkeley, California 94720, USA

THE apparent emptiness of the outer Solar System has been a long-standing puzzle for astronomers, as it contrasts markedly with the abundance of asteroids and short-period comets found closer to the Sun. One explanation for this might be that the orbits of distant objects are intrinsically short-lived, perhaps owing to the gravitational influence of the giant planets. Another possibility is that such objects are very faint, and thus they might easily go undetected. An early survey[1] designed to detect distant objects culminated with the discovery of Pluto. More recently, similar surveys yielded the comet-like objects 2060 Chiron[2] and 5145 Pholus[3] beyond the orbit of Saturn. Here we report the discovery of a new object, 1992 QB_1, moving beyond the orbit of Neptune. We suggest that this may represent the first detection of a member of the Kuiper belt[4,5], the hypothesized population of objects beyond Neptune and a possible source of the short-period comets[6-8].

Our observations are part of a deep-imaging survey[9] of the ecliptic, made with the University of Hawaii 2.2-m telescope on Mauna Kea. The survey uses Tektronix $1{,}024 \times 1{,}024$ pixel and $2{,}048 \times 2{,}048$ pixel charge-coupled devices (CCDs) at the $f/10$ Cassegrain focus. Both CCDs have anti-reflection coatings which yield quantum efficiencies of ~90% at wavelength $\lambda \approx 7{,}000$ Å (K. Jim, personal communication). Survey observations are obtained in sets of four images per field with a total timebase of 2 or more hours. Each image is exposed for 900 s while autoguiding at sidereal rate. Because objects in the outer Solar System have small proper motions, our survey was optimized to detect slowly moving objects (SMOs). The angular motions of SMOs are sufficiently small that little trailing-loss results from sidereal tracking. This strategy is found to provide optimum sensitivity to the linear, correlated motion expected of slowly moving objects. By restricting observations to stellar images of full width at *half* maximum (FWHM) ≤ 1.0 arcsec, and to moonless skies, we obtain limiting magnitudes $m_R \sim 25$. To date, a

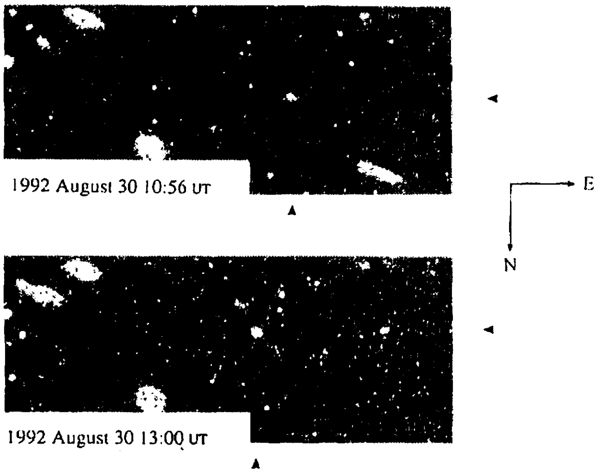

FIG. 1 Discovery images of 1992 QB_1 (marked by arrows), obtained UT 1992 August 30 at the University of Hawaii 2.2-m telescope, using a Mould R filter (central wavelength $\lambda_c = 6{,}500$ Å, FWHM $\Delta\lambda = 1{,}250$ Å). The images show regions of a 2,048 × 2,048 pixel Tektronix CCD (each pixel subtends 0.22 arcsec). Stellar images are about 0.8 arcsec FWHM. The elongated object to the lower right in the top image is a main-belt asteroid: it appears in the top left of the bottom image and demonstrates the extraordinarily slow motion of 1992 QB_1. The field shown is ~90 arcsec in width.

sky area of 0.7 square degrees has been imaged to this depth. We are extending our coverage to 1 square degree.

We confine our observations to the opposition direction, where the angular motion of distant objects is retrograde and primarily due to the Earth's motion. At opposition, the parallactic angular motion $\dot{\theta}$ (arcsec per hour) is given by $\dot{\theta} = 148[(1 - R^{-1/2})/(R-1)]$, where R (in astronomical units, AU) is the heliocentric distance[9]. Thus, a measurement of $\dot{\theta}$ yields R directly. Our observations are restricted to the spring and autumnal equinoxes to benefit further from the large galactic latitude of the opposition point, and from the resultant low density of background stars. In fact, field galaxies pose a worse contamination problem than do field stars in our observations.

The object 1992 QB_1 was detected in real time on UT 1992 August 30 (ref. 10). The discovery images are shown in Fig. 1, where the faster motion of a nearby, unnumbered main-belt asteroid emphasizes the remarkably small angular motion (and hence large distance) of QB_1. The slow motion of the SMO (2.6 arcsec h^{-1} west and 1.1 arcsec h^{-1} south) was confirmed on UT August 31 and September 01. Absence of detectable diurnal parallax confirmed that the object was not a near-Earth asteroid whose proper motion fortuitously resembled that of a SMO. Positions of 1992 QB_1 were obtained with reference to stars in the Hubble Guide Star Catalogue. Measurements relative to these stars suggested an absolute astrometric accuracy of ±1 arcsec, and the relative positions were precise to about ±0.3 arcsec. Astrometric positions were communicated to B. Marsden at the Center for Astrophysics. Follow-up astrometry from the 2.2-m telescope was obtained on UT 1992 September 25, and other observers have reported astrometric measurements in the following three months[11-13]. Observations from 1992 August 30 to December 25 yielded a current heliocentric distance $R \approx 41$ AU, and were used to calculate the orbital parameters listed in Table 1 (ref. 13).

At distance $R = 41$ AU, geocentric distance $\Delta = 40$ AU and phase angle $\alpha = 0.5°$, the apparent red magnitude $m_R = 22.8 \pm 0.2$ on August 30 corresponds to absolute magnitude $H_R = 6.6 \pm 0.2$. For comparison, the absolute magnitude of the distant comet 2060 Chiron in its faint state is $H_R \approx 6.3 \pm 0.1$ (ref. 14). Lacking a measurement of the albedo, we cannot determine the size of 1992 QB_1. However, an albedo $p_R = 0.04$, similar to that of a comet nucleus, suggests a diameter $d \approx 250$ km, roughly one-eighth the size of Pluto. The Kron-Cousins colours of 1992 QB_1

TABLE 1 Preliminary orbital parameters

Semi-major axis	a	44.4 AU
Eccentricity	e	0.11
Inclination	i	2.2°
Orbital period	P	296 years
Perihelion date	T	AD 2023
Perihelion distance	q	39.6
Aphelion distance	Q	49.1

Based on astrometry in the interval 1992 August 30 to December 25. Orbit solution is by Marsden[13].

were measured on UT 1992 August 30 and September 01. Our best estimates are $m_V - m_R = 0.6 \pm 0.1$ and $m_R - m_I = 1.0 \pm 0.2$, to be compared with solar colours $m_V - m_R = 0.32$ and $m_R - m_I = 0.4$, respectively. Here m_V, m_R and m_I are the stellar magnitudes measured with V (5,500 Å), R (6,500 Å) and I (8,000 Å) filters. The $m_R - m_I$ colour is based on a single I filter image. Nevertheless, it seems that 1992 QB_1 is substantially redder than sunlight, inconsistent with a surface of pure ice but consistent with dirty ice, or one contaminated with organic compounds. For comparison, the corresponding colours of the distant object 5145 Pholus are $m_V - m_R \approx 0.7$ and $m_R - m_I \approx 0.7$ (ref. 15), and all other known cometary nuclei are substantially less red[16]. Both Pholus and 1992 QB_1 may retain primitive organic mantles produced by prolonged cosmic-ray irradiation. Such mantles would be disrupted or buried by rubble mantles on active, near-Sun comets[15,16].

Figure 2 shows the surface brightness profile measured from images taken UT 1992 September 01. The profile of a nearby field star is shown for comparison. Figure 2 supplies no evidence for a resolved coma down to surface brightness 29 mag per square arcsec, at a distance of 1.5 arcsec from the centre of the image. The absence of resolved coma allows us to place a model-dependent limit on the mass loss rate from 1992 QB_1, using a profile-fitting method[17]. This limit is $dm/dt < 0.7$ kg s^{-1}, so 1992 QB_1 is at least 10^4 times less active than a Halley-class, near-Sun comet and probably less active than 2060 Chiron ($dm/dt \approx 1$ kg s^{-1})[18]. Weaker activity cannot be constrained by existing observations, however.

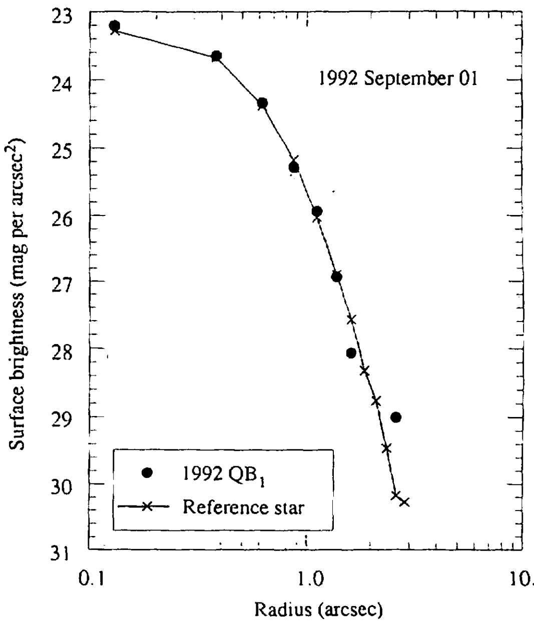

FIG. 2 Surface brightness profile of 1992 QB_1 measured UT 1992 September 01 with 0.8 arcsec FWHM images. The profile was computed from four separate R-filter images of total integration time 3,600 s. A scaled profile of a nearby field star is shown for reference. The image of 1992 QB_1 is consistent with a point source down to surface brightness ~29 magnitudes per square arcsec.

As our survey is still in progress, we will not discuss in detail the statistics implied by the detection of 1992 QB_1. It is, however, interesting to make a crude estimate of the Kuiper belt population. We note that 1992 QB_1 was detected in a survey that has so far covered 0.7 square degree. The implied surface density of similar objects is of order 1 per square degree. The inclination of 1992 QB_1 is 2 degrees (Table 1), so the angular width of the belt is at least 4 degrees, and is presumably much larger. A lower limit to the projected area of the Kuiper belt is $360 \times 4 = 1{,}440$ square degree, and the number of similar objects is thus $N \geq 1{,}440$. A minimal belt mass, based on an assumed diameter of 250 km and density of 10^3 kg m^{-3} for each object, is $M \geq 1 \times 10^{22}$ kg $\approx 2 \times 10^{-3}$ $M_{\rm Earth}$ (about 1 Pluto mass). This is compatible with the upper limit to the belt mass inferred from dynamical observations of P/Halley, $M \approx 1$ $M_{\rm Earth}$ (refs 19–21), and with the minimal mass needed to supply the observed flux of short period comets, $M \approx 0.02$ $M_{\rm Earth}$ (ref. 6). The estimated mass must be augmented to account for Kuiper belt comets too small or too distant to be detected in the present survey, but this depends on the (poorly known) mass and spatial distribution of cometary nuclei. M is a lower limit to the true mass.

The faintness of 1992 QB_1 makes it unlikely that earlier observations will be identified, so limiting the accuracy of the derived orbital parameters. The astrometric timebase used to obtain the parameters in Table 1 is only 10^{-3} of the orbit period. Although these parameters are not finalized, it is likely that the perihelion lies beyond the orbits of the gas giant planets (the expected perihelion $q \approx 40$ AU, compared with the Neptune aphelion $Q_N = 30.3$ AU)[13]. It thus seems that 1992 QB_1 escapes strong planetary perturbations and is, in this sense, more primitive than its presumed cousins at smaller distances, 2060 Chiron and 5145 Pholus. Theory suggests that, although many orbits between the giant planets are unstable on timescales short compared with the age of the Solar System, orbits beyond Neptune may be stable for longer times[22-27]. In particular, low-eccentricity orbits with semi-major axes of ~44 AU (Table 1) have lifetimes in excess of 10^9 yr (ref. 27), supporting the idea that 1992 QB_1 is a Kuiper belt comet.

Note added in proof: On UT 1993 March 28 we detected a second slow moving object (*IAU Circ.* 5370, 29 March 1993). This object, 1993 FW, has the same magnitude and angular motion as 1992 QB_1, and is presumably also resident in the Kuiper belt. Our detection of 1993 FW supports the Kuiper belt population estimate given above. □

Received 13 January: accepted 30 March 1993.

1. Tombaugh, C. W. in *Planets and Satellites* (eds Kuiper G. P. & Middlehurst, B. M.) 12–30 (Univ. Chicago Press, Chicago, 1961).
2. Kowal, C., Liller, W. & Marsden, B. in *Dynamics of the Solar System, Proc. IAU Symp.* No. 81 (ed. Duncombe R.) 245–249 (Reidel, Dordrecht, 1979).
3. Scottie, J. V. *IAU Circ.* No. 5434 (1992).
4. Edgworth, K. E. *Mon. Not. R. astr. Soc.* **109**, 600–609 (1949).
5. Kuiper, G. P. in *Astrophysics* (ed. Hynek, J. A.) 357–424 (New York, McGraw-Hill, 1951).
6. Duncan, M., Quinn, T. & Tremaine, S. *Astrophys. J.* **328**, L69–L73 (1988)
7. Whipple, F. *Proc. Nat. Acad. Sci.* **51**, 711–717 (1964).
8. Fernandez, J. A. *Mon. Not. R. astr. Soc.* **192**, 481–491 (1980).
9. Luu, J. X. & Jewitt, D. C. *Astr. J.* **95**, 1256–1262 (1988).
10. Jewitt, D. C. & Luu, J. X. *IAU Circ.* No. 5611 (1992).
11. McNaught, R. & Steel, D. *Minor Planet Circ.* 20878 (1992)
12. Hainault, O. & Elst, E. *Minor Planet Circ.* 20902 (1992).
13. Marsden, B. G. *IAU Circ.* No. 5684 (1992).
14. Luu, J. X. & Jewitt, D. C. *Astr. J.* **100**, 913–932 (1990).
15. Mueller, B., Tholen, D., Hartmann, W. & Cruikshank, D. *Icarus* **97**, 150–154 (1992).
16. Jewitt, D. C. *Cometary Photometry* in *Comets in the Post-Halley Era* (ed. Newburn, R.) 19–65 (Kluwer, Dordrecht, 1990).
17. Luu, J. X. & Jewitt, D. C. *Icarus* **97**, 276–287 (1992).
18. Luu, J. X. & Jewitt, D. C. *Astr. J.* **100**, 913–932 (1990).
19. Hamid, S. E., Marsden, B. & Whipple, F. *Astr. J.* **73**, 727–729 (1968).
20. Yeomans, D. K. *Proc. 20th ESLAB Symp.* 419–425 (ESA SP-250, Heidelberg, 1986)
21. Hogg, D. W., Quinlan, G. D. & Tremaine, S. *Astr. J.* **101**, 2274–2286 (1991).
22. Torbett, M. V. *Astr. J.* **98**, 1477–1481 (1989).
23. Torbett, M. V. & Smoluchowski, R. *Nature* **345**, 49–51 (1990).
24. Quinn, T., Tremaine, S. & Duncan, M. *Astrophys. J.* **355**, 667–679 (1990).
25. Duncan, M. & Quinn, T. in *Protostars and Planets III* (Tucson, in the press).
26. Holman, M. J. & Wisdom, J. *Astr. J.* (in the press).
27. Levison H. & Duncan, M. *Astrophys. J.* (in the press)

ACKNOWLEDGEMENTS. We thank B. Marsden for discussions about 1992 QB_1, G. Luppino for CCD cameras, the Institute for Astronomy TAC for consistent allocation of time to this project, and A. Pickles for obtaining supporting astrometric images. The Planetary Astronomy program of NASA provides financial support at the UH 2.2-m telescope. J.X.L. is in receipt of a Hubble Fellowship.

Dust particle impacts during the Giotto encounter with comet Grigg–Skjellerup

J. A. M. McDonnell[*], N. McBride[*], R. Beard[*], E. Bussoletti[†], L. Colangeli[‡], P. Eberhardt[§], J. G. Firth[||], R. Grard[¶], S. F. Green[*], J. M. Greenberg[*], E. Grün[**], D. W. Hughes[††], H. U. Keller[‡‡], J. Kissel[**], B. A. Lindblad[§§], J.-C. Mandeville[||||], C. H. Perry[||], K. Rembor[¶¶], H. Rickman[**], G. H. Schwehm[¶], R. F. Turner[||], M. K. Wallis[***] & J. C. Zarnecki[*]

* Unit for Space Sciences, Physics Laboratory, University of Kent, Canterbury, Kent CT2 7NR, UK
† Istituto di Fisica Sperimentale, Istituto Universitario Navale, Via A. De Gasperi 5, 80133 Napoli, Italy
‡ University of Cassino, Via Zamosch 43, 03043 Cassino (Fr), Italy
§ Physikalisches Institut, Universität Bern, CH-3012 Bern, Sidlerstrasse 5, Switzerland
|| Space Science Department, Rutherford Appleton Laboratory, Chilton, Didcot OX11 0QX, UK
¶ PSS, ESTEC, Postbus 299, 2200 AG Noordwijk, Netherlands
* Rijksuniversiteit te Leiden, Huygens Laboratorium, Postbus 9504, 2300 RA Leiden, Netherlands
** Max-Planck-Institut für Kernphysik, D-6900 Heidelberg, Germany
†† Department of Physics, University of Sheffield, Sheffield S3 7RH, UK
‡‡ Max Planck Institut für Aeronomie, D-3411 Katlenburg-Lindau, Germany
§§ Lund Observatory, Box 43, S-221 00 Lund, Sweden
|||| ONERA-CERT-DERTS, BP No. 4025 31055 Toulouse Cedex, France
** Astronomical Observatory, Box 515, S-751 20 Uppsala, Sweden
¶¶ Fakultät für Physik, Universität Karlsruhe, D-7500 Karlsruhe, Germany
*** School of Mathematics, University of Wales, Senghennydd Road, Cardiff CF2 4AG, UK

IN the European Space Agency's 1992 Giotto Extended Mission, the Dust Impact Detection System operated successfully during a fly-by that took the spacecraft within about 200 km of the nucleus of comet Grigg–Skjellerup. During the encounter, three meteoroid impacts were detected on Giotto's front shield. The particle masses were found to be 100^{+105}_{-50} μg, 2^{+4}_{-1} μg and 20^{+25}_{-10} μg, suggesting that the mass distribution of the cometary dust was dominated by larger particles. This is supported by the independent detection of a very large meteoroid (14^{+40}_{-4} mg) by the Giotto Radio-Science Experiment, and is consistent with data over the same mass range from the 1986 encounter with comet Halley. The results indicate a higher rate of mass loss from the nucleus than previously thought, and hence a higher dust-to-gas mass ratio.

The Dust Impact Detection System (DIDSY) was designed to measure the flux of dust particles in the mass range 10^{-19} kg to $>10^{-6}$ kg in the coma of comet Halley (Fig. 1, refs 1 and 2). The DID1 IMP-P sensor suffered impact damage at the Halley encounter, and at Grigg-Skjellerup, the instrument was noisy and gave no interpretable results. The DID1 IPM-M sensor, however, was fully operational. The DID7 CIS sensor also suffered impact degradation at Halley, and was largely non-operational. The piezoelectric momentum sensors (DID2 to 5) were fully operational.

The 1986 Halley encounter geometry was such that particles struck the front shield at normal incidence with relative velocity 68.4 km s^{-1}. A hypervelocity particle having momentum mv will transfer momentum εmv to the shield (the enhancement is due to target ejecta) where ε is the momentum enhancement factor. The value taken at Halley[3] was $\varepsilon = 11$. At Grigg-Skjellerup the trajectories of particles striking the shield made a 21.2° angle with the shield at a relative velocity of 13.8 km s^{-1}. These factors reduced ε considerably. Experiments using the 2-MV dust accelerator at the Unit for Space Sciences, Kent, yield a value of $\varepsilon = 3.1 \pm 1.0$. This reduced value of ε raises the piezoelectric